# Doxorubicin-Loaded Alginate-*g*-Poly(*N*-isopropylacrylamide) Micelles for Cancer Imaging and Therapy

Dong-Gyun Ahn,[†] Jangwook Lee,[†] So-Young Park,[‡] Young-Je Kwark,[‡] and Kuen Yong Lee*,[†]

[†]Department of Bioengineering, Hanyang University, Seoul 133-791, Republic of Korea
[‡]Department of Organic Materials and Fiber Engineering, Soongsil University, Seoul 156-743, Republic of Korea

S *Supporting Information*
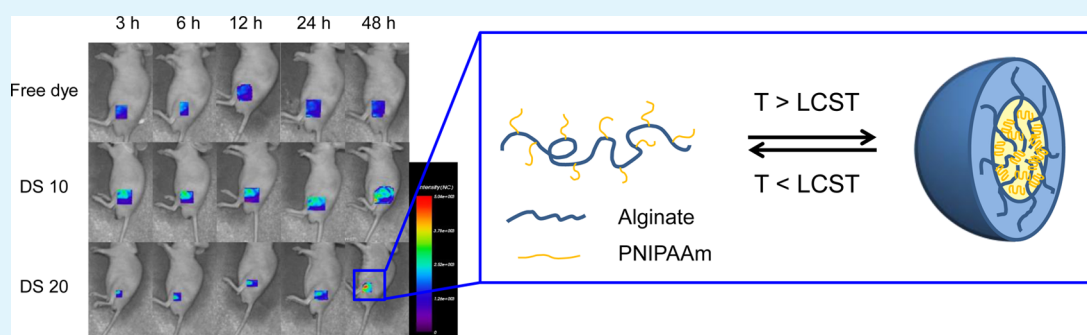
ABSTRACT: Chemotherapy is a widely adopted method for the treatment of cancer. However, its use is often limited due to side effects produced by anti-cancer drugs. Therefore, various drug carriers, including polymeric micelles, have been investigated to find a method to overcome this limitation. In this study, alginate-based, self-assembled polymeric micelles were designed and prepared using alginate-g-poly(*N*-isopropylacrylamide) (PNIPAAm). Amino-PNIPAAm was chemically introduced to the alginate backbone via carbodiimide chemistry. The resulting polymer was dissolved in distilled water at room temperature and formed self-assembled micelles at 37 °C. Characteristics of alginate-*g*-PNIPAAm micelles were dependent on the molecular weight of PNIPAAm, the degree of substitution, and the polymer concentration. Doxorubicin (DOX), a model anti-cancer drug, was efficiently encapsulated in alginate-*g*-PNIPAAm micelles, and sustained release of DOX from the micelles was achieved at 37 °C in vitro. These micelles accumulated at the tumor site of a tumor-bearing mouse model as a result of the enhanced permeability and retention effect. Interestingly, DOX-loaded alginate-*g*-PNIPAAm micelles showed excellent anti-cancer therapeutic efficacy in a mouse model without any significant side effects. This approach to designing and tailoring natural polymer-based systems to fabricate nanoparticles at human body temperature may provide a useful means for cancer imaging and therapy.

KEYWORDS: *micelle, alginate, cancer, diagnosis, therapy*

INTRODUCTION

Nanoparticle systems have been attractive to many biomedical science and engineering areas and have recently shown great potential, especially in molecular imaging, drug, and gene delivery applications.[1−4] One typical method to fabricate nanoparticles is the use of self-assembly systems, such as amphiphilic polymers. Self-assembled polymeric nanoparticles have recently attracted much attention as potential carriers for drug delivery[5,6] due to their unique and stable core−shell structure having a small size and narrow size distribution.[7,8] Furthermore, they can efficiently incorporate hydrophobic anti-cancer drugs into the inner hydrophobic core under aqueous conditions without a toxic solvent or detergent.[9,10] Drug-loaded nanoparticles have been shown to have an increased circulation time in the body and passive accumulation at the tumor site due to the enhanced permeability and retention (EPR) effect.[11]

Various polymeric materials can be used to develop self-assembled structures. In our study, alginate was chosen as a base material. Alginate is a widely used biomaterial derived from brown seaweed; it has many useful biomedical applications due to its excellent biocompatibility, low toxicity, and relatively low cost.[12] In addition, alginate displays poor interaction with proteins, which may be beneficial as a systemic delivery vehicle in the body. To date, alginate has attracted much attention as a delivery vehicle for cancer therapy.[13,14] However, alginate-based systems typically require ionic cross-linking[15−17] using divalent cations (e.g., Ca^{2+}), which may be disintegrated in the body due to the abundance of monovalent ions, such as sodium ions, under physiological conditions.[12]

Temperature-induced micelle formation using amphiphilic polymers has been widely investigated for its utility in nanoparticle preparation.[18−21] Alginate, however, is not
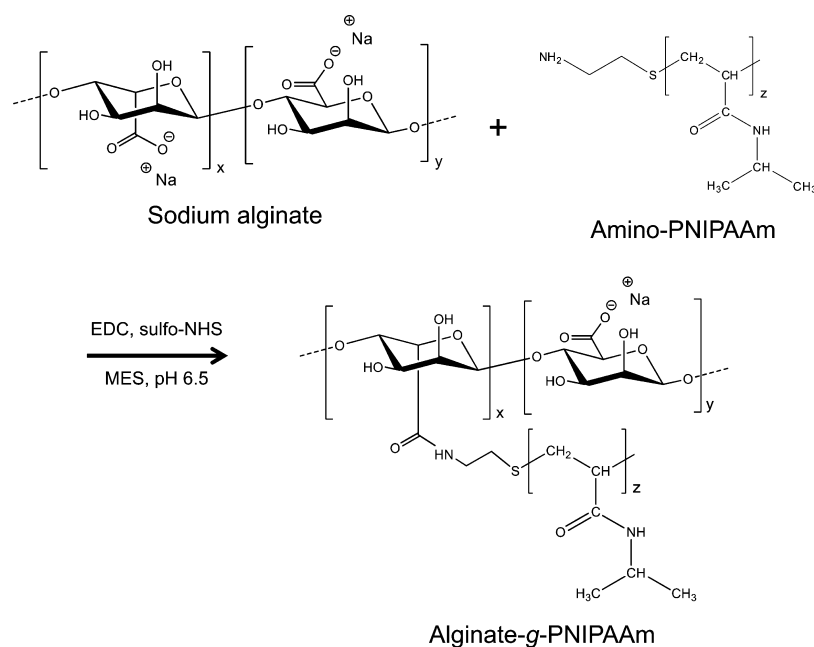
Figure 1. Synthetic scheme for the chemical conjugation of amino-PNIPAAm to alginate via carbodiimide chemistry.

temperature-responsive in physiological environments. Poly(*N*-isopropylacrylamide) (PNIPAAm) is a well-known temperature-responsive polymer, and its hydrophobicity can be increased or decreased by simply changing the temperature; this process is also reversible.[22,23] The temperature at which hydrophilic−hydrophobic transition behavior occurs is called the lower critical solution temperature (LCST). Generally, the LCST of PNIPAAm is accepted to be 32 °C.[24,25] The combination of alginate and PNIPAAm enables hydrogel formation with temperature/pH sensitivity that is useful for many biomedical applications.[26−29] However, studies on micelle formation using alginate and PNIPAAm are still lacking. PNIPAAm has found useful applications as a hydrophobic group in polymer amphiphiles above the LCST, and poly(2-carboxyethyl-2-oxazoline)[30] or poly(ethylene oxide)[31] was used as a hydrophilic segment. Micelle formation of these amphiphilic polymers was confirmed above the LCST, and these micelles can incorporate a hydrophobic drug only above the LCST.[32]

We thus hypothesized that alginate modified with PNIPAAm could form self-assembled micelles at human body temperature and that these systems could be useful as a drug carrier for cancer therapy. Amphiphilic alginate-*g*-PNIPAAm was synthesized by the conjugation of amino-PNIPAAm to the alginate backbone by carbodiimide chemistry, and various characteristics of alginate-*g*-PNIPAAm micelles were investigated. Doxorubicin (DOX) was chosen as a model anti-cancer drug and incorporated into the polymeric micelles. DOX is one of the most frequently used anti-cancer drugs for clinical treatment of major organ carcinoma (e.g., breast, stomach, lung, ovary, and bladder) and soft tissue sarcoma.[25] However, its clinical applications are often limited due to its severe side effects, such as cardiotoxicity and heart failure.[25,33] To overcome this limitation, various delivery systems for DOX have been reported to reduce its side effects and also to improve its therapeutic efficacy.[34,35] The release behavior of DOX from alginate-based micelles was monitored in vitro. The distribution of alginate-*g*-PNIPAAm micelles tagged with near-

infrared fluorescence dye was investigated using a tumor-bearing mouse model; the model also assessed the therapeutic efficacy of DOX-loaded micelles.

■ EXPERIMENTAL SECTION

Materials. Sodium alginate (low viscosity), 1-ethyl-3-(dimethylaminopropyl) carbodiimide (EDC), pyrene, *N*,*N*-dimethylformamide (DMF), diethyl ether, tetrahydrofuran (THF), 2-(*N*-morpholino)-ethanesulfonic acid (MES), triethylamine (TEA), dimethyl sulfoxide (DMSO), deuterium oxide (D$_2$O), *N*-isopropylacrylamide (NIPAAm), cysteamine hydrochloride (CAH), and azobis(isobutyronitrile) (AIBN) were purchased from Sigma-Aldrich (St. Louis, MO, USA). Phosphate buffered saline (PBS), RPMI-1640 culture media, and fetal bovine serum (FBS) were supplied by Gibco (Grand Island, NY, USA). *N*-Hydroxysulfosuccinimide (sulfo-NHS) was obtained from Thermo Scientific (Pittsburgh, PA, USA), and EZ-Cytox was supplied by DoGen (Seoul, Korea). DOX and FCR-675 amine were purchased from LC Laboratories (Woburn, MA, USA) and BioActs (Incheon, Korea), respectively. Orient Bio (Seongnam, Korea) provided the immunodeficient mice.

Synthesis of Amino-Poly(*N*-isopropylacrylamide). Amine-terminated poly(*N*-isopropylacrylamide) (A-PNIPAAm) was prepared by radical polymerization using CAH as a chain-transfer agent.[24] NIPAAm (8.84 × 10^{-2} mol), CAH (1.47 × 10^{-2} mol), and AIBN (1.41 × 10^{-2} mol) were dissolved in 30 mL of DMF. After degassing the solution using a freeze−thaw method, polymerization was carried out at 70 °C for 6 h. Upon completion, the product was precipitated using an excess of diethyl ether and then dried in a vacuum oven at room temperature. The dried polymer was purified by repeated precipitation in hot water followed by freeze-drying. The molecular weight of A-PNIPAAm was determined using gel permeation chromatography (Waters; Milford, MA, USA) equipped with a series of Mixed C columns (Polymer Laboratories; Santa Clara CA, USA) and a refractive index detector. DMF was used as the mobile phase, and the columns were calibrated according to poly(ethylene oxide) calibration standards with narrow polydispersity (Polymer Standards Service; Amherst, MA, USA).

Synthesis and Characterization of Alginate-*g*-PNIPAAm. Alginate-*g*-PNIPAAm was synthesized via carbodiimide chemistry (Figure 1).[36] Alginate (1 g) and A-PNIPAAm were dissolved in MES buffer (pH 6.5, 10 mg/mL), and EDC (27.40 mg), sulfo-NHS (48.42 mg), and PNIPAAm were added to the alginate solution sequentially

followed by vigorous stirring for 20 h at 4 °C. Once the reaction was complete, the mixture was loaded into a dialysis bag (molecular weight cutoff: 12 000 to 14 000) and dialyzed against distilled water for 4 days to remove any residual reagents and byproducts. After dialysis, the solution was lyophilized. Conjugation between alginate and PNIPAAm was confirmed by Fourier transform infrared spectroscopy (Nicolet 6700, Thermo Scientific; Pittsburgh, PA, USA) in the wavenumber range of 400−4000 cm^{-1}. ^{1}H NMR spectroscopy was also used to verify the conjugation (VNMRS 600 MHz, Varian; Palo Alto, CA, USA). Samples were dissolved in D$_2$O at a 10 mg/mL concentration to obtain the NMR spectra. The degree of substitution (DS), defined as the number of conjugated PNIPAAm per 100 saccharide units of alginate, was determined from elemental analysis (Flash EA1112, Thermo Finnigan; San Joes, CA, USA) and varied in the range from 5 to 20. The number immediately following DS indicates the mole ratio between PNIPAAm and 100 saccharide units of alginate initially used for the synthesis of alginate-g-PNIPAAm.

Size and Morphology of Alginate-g-PNIPAAm Micelles. Alginate-g-PNIPAAm was dissolved in PBS with gentle shaking, and the solution was placed in an incubator at 37 °C for 48 h before use. The size of the alginate-g-PNIPAAm micelles was determined by dynamic light scattering (DLS) using a zetasizer (Nano ZS, Malvern Instruments; Malvern, UK). Thermoreversible micelle formation was also confirmed using the zetasizer by changing the temperature. The surface morphology of alginate-g-PNIPAAm micelles was investigated using field-emission scanning electron microscopy (S-4800 UHR FE-SEM, Hitachi; Tokyo, Japan). In brief, the micelle solution was quickly frozen using liquid nitrogen, freeze-dried, and then coated with platinum under vacuum before the images were obtained.

Determination of the Critical Micelle Concentration. The critical micelle concentration (CMC) value of alginate-g-PNIPAAm was determined by fluorescence spectroscopy using pyrene. Pyrene was dissolved in THF and diluted with distilled water (12×10^{-7} M). After the THF was evaporated overnight, the solution was added to an aqueous alginate-g-PNIPAAm solution with concentrations ranging from 1.0×10^{-5} to 4.0 mg/mL ([pyrene] = 6.0×10^{-7} M). The excitation wavelength was 310 nm, and emission spectra were recorded using a fluorescence spectrometer (Spectrometer F-7000, Hitachi; Tokyo, Japan). The slit widths for emission and excitation were set at 2 and 0.5 nm, respectively. The intensity ratio (I_1/I_3) of the first (375 nm) and the third (386 nm) highest peaks in the emission spectra of pyrene was utilized to determine the CMC value.

Cytotoxicity of Alginate-g-PNIPAAm. Cytotoxicity of alginate-g-PNIPAAm was evaluated by WST-based assay (EZ-Cytox). Squamous cell carcinoma (SCC7) cells were seeded onto 96-well tissue culture plates (5×10^3 cells/well) and cultured in RPMI 1640 media (10% FBS, 1% penicillin−streptomycin) in a 5% CO$_2$ atmosphere at 37 °C. After 24 h of incubation, the alginate-g-PNIPAAm solution was added to each well, and the cells were incubated for another 24 h. Once the incubation was complete, the cells were treated with 10 μL of EZ-Cytox at 37 °C for 2 h. The absorbance was measured at 450 nm using a UV–vis spectrophotometer (SpectraMax M2^e, Molecular Devices; Sunnyvale, CA, USA).

Preparation of Doxorubicin-Loaded Alginate-g-PNIPAAm Micelles. DOX was dissolved in DMF (2 mg/mL), and TEA (five times the molar quantity of DOX) was added to the DOX solution. The solution was allowed to react for 20 h with stirring. Alginate-g-PNIPAAm (0.5 mg) was dissolved in distilled water (0.9 mL), and the DOX solution (0.1 mL) was added to the polymer solution. DOX-loaded micelles were prepared by raising the temperature of the mixture solution from room temperature to 37 °C for 5 min. Then, the mixed solution was transferred to a dialysis bag (molecular weight cutoff: 6000−8000) and dialyzed against distilled water for 3 h at 37 °C to remove unloaded DOX.

In Vitro Drug Release. The DOX release from alginate-g-PNIPAAm micelles was investigated in vitro by a dialysis-diffusion method. Briefly, 1 mL of the DOX-loaded micelle solution was transferred to a dialysis bag (molecular weight cutoff: 6000 to 8000) and dialyzed against distilled water. The cumulative DOX release was monitored at predetermined time intervals (0.5, 1, 3, 6, 12, 24, 48, 72,

and 96 h) under sink conditions. The concentration of the released DOX was determined using fluorescence spectroscopy (λ_{ex} = 470 nm; λ_{em} = 590 nm).

In Vivo Biodistribution and Tumor Targeting Ability of Alginate-g-PNIPAAm Micelles. Five-week-old male mice were anesthetized with an intraperitoneal injection of Zoletil (35 mg/kg) and Rompun (2 mg/kg). Tumor-bearing mice were established by the subcutaneous inoculation of SCC7 cells (1.0×10^6 per mouse) onto the back of the mice. When the tumor volume reached about 200 mm^3, dye-conjugated alginate-g-PNIPAAm micelles were intravenously injected into the mice (7.5 mg/kg). The dye-conjugated alginate-g-PNIPAAm was prepared by chemically coupling FCR-675 amine to alginate-g-PNIPAAm via carbodiimide chemistry (MES buffer; pH 6.5; 1 mg/mL; polymer/dye = 25, weight ratio). All of the procedures were in compliance with Hanyang University guidelines for the care and use of laboratory animals.

The tumor accumulation profiles were assessed using the eXplore Optix system (Advanced Research Technologies, Montreal, Canada). Laser power and count time settings were optimized at 10 μW and 0.3 s per point, respectively. The laser diode was used at a wavelength of 670 nm to excite FCR-675 amine. Near-infrared fluorescence (NIRF) emission at 700 nm was detected with a fast photomultiplier tube (Hamamatsu, Japan) and a time-correlated single-photon counting system (Becker and Hickl, Berlin, Germany). To investigate the biodistribution of dye-conjugated alginate-g-PNIPAAm micelles in the tumor-bearing mouse model, major organs and tumors were dissected from the mice 48 h postinjection. NIRF images of the organs and tumors were taken using a 12-bit CCD camera (Kodak Image Station 4000 MM, Kodak; New Haven, CT, USA) equipped with a special C-mount lens and a Cy5.5 bandpass emission filter (680−720 nm). The NIRF intensity was calculated using the region of interest (ROI) function of the Analysis Workstation software (Advanced Research Technologies).

Anti-cancer Efficacy of DOX-Loaded Alginate-g-PNIPAAm Micelles in Tumor-Bearing Mice. Tumor-bearing mice were prepared as previously described, and DOX-loaded alginate-g-PNIPAAm micelles with different DS were intravenously injected when the tumor volume reached about 200 mm^3 ([DOX] = 1.2 mg/kg mouse; five total injections at days 0, 2, 4, 6, and 8; n = 5). Saline and free DOX were also intravenously injected at days 0, 2, 4, 6, and 8 as controls. Changes in tumor volume and body weight were monitored for 2 weeks. The mice were sacrificed at 2 weeks after the first injection, and the tumor tissues were collected, embedded into optimal cutting temperature compound (TISSUE-TEK OCT compound, Sakura Finetek, Tokyo, Japan), and frozen at −70 °C. The frozen tissue samples were cut into 10 μm thick sections at −20 °C and stained with hematoxyline and eosin (H&E). Cellular apoptosis in the tissue section was identified using an apoptosis detection kit (ApopTagRed In Situ, Millipore, Billerica, MA, USA) according to the manufacturer's protocol.

Statistical Analysis. All data are presented as mean ± standard deviation. Statistical analyses were performed using Student's t test. A value of $p < 0.05$ was considered to be statistically significant.

■ RESULTS AND DISCUSSION

Synthesis and Characterization of Alginate-g-PNIPAAm. Radical polymerization using CAH as a chain-transfer agent was used to synthesize PNIPAAm that contained an amine group at the end of the chain (A-PNIPAAm). An amino group can be introduced to the end of the PNIPAAm chain due to the high chain-transfer constant of the thiol groups in CAH.[24] The number-average molecular weights of A-PNIPAAm (MW$_{PNIPAAm}$) used in this study were 1400 (1 kDa), 2600 (2 kDa), and 4000 g/mol (4 kDa). Next, A-PNIPAAm was chemically coupled to the alginate backbone via carbodiimide chemistry. Conjugation between the amino groups of A-PNIPAAm and the carboxylic groups of alginate was confirmed by FT-IR spectroscopy (Figure S1). The
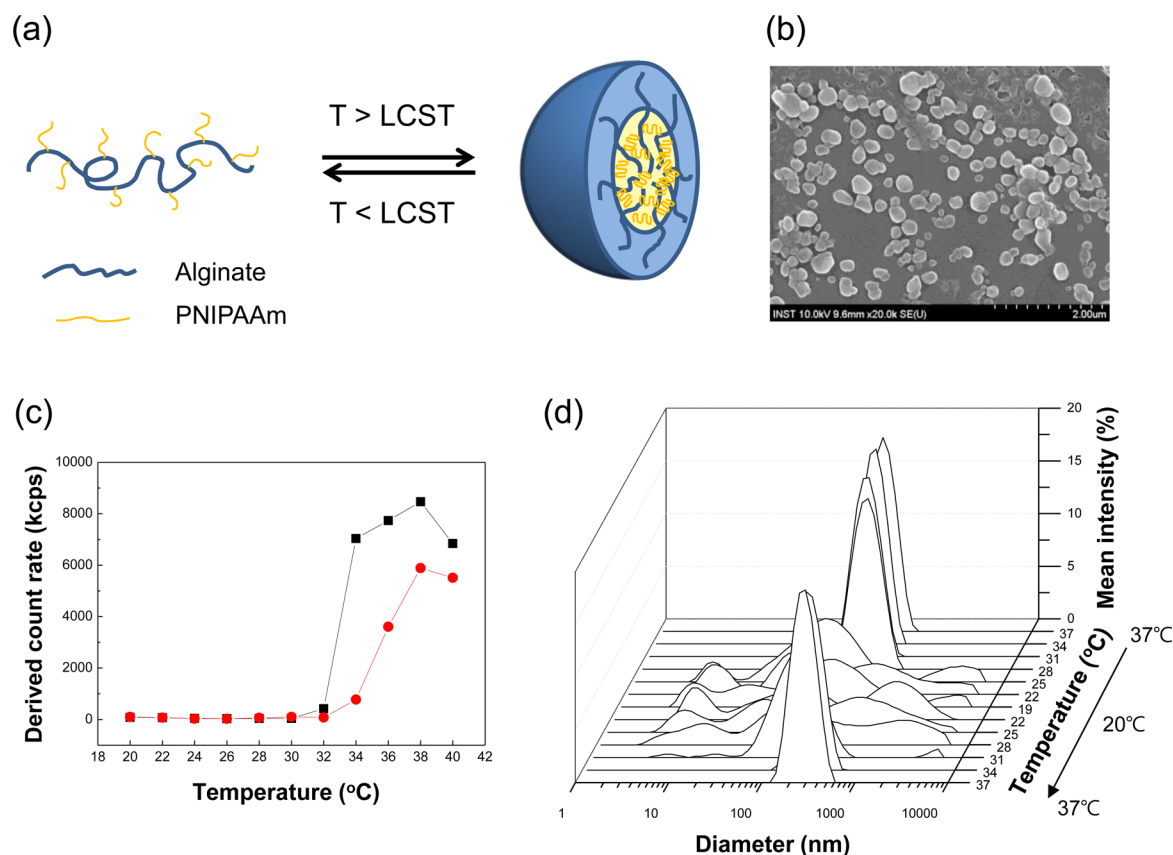
22071

dx.doi.org/10.1021/am505444c | ACS Appl. Mater. Interfaces 2014, 6, 22069−22077

Figure 2. (a) Schematic of thermally reversible alginate-*g*-PNIPAAm micelle formation and (b) morphology of the micelles observed by scanning electron microscopy ([polymer] = 0.1 mg/mL; MW$_{PNIPAAm}$ = 1 kDa, DS 5). (c) Changes in the light scattering intensity of A-PNIPAAm (■) and alginate-*g*-PNIPAAm (●) dissolved in distilled water as a function of temperature. (d) Multiple plots of the size distribution of alginate-*g*-PNIPAAm micelles at different temperatures. Each plot was collected every 3 °C.

presence of the aminoethyl end groups of A-PNIPAAm was confirmed by FT-IR, which showed two characteristic primary amine peaks at 3280 and 3450 cm^{-1}. Alginate-*g*-PNIPAAm produced new absorption peaks of amide bonds at 1623 cm^{-1} (C=O stretch) and 1541 cm^{-1} (N−H bend).

Conjugation between alginate and PNIPAAm was also confirmed by ^{1}H NMR (Figure S2). Alginate is a linear polysaccharide composed of *β*-D-mannuronate (M) and *α*-L-guluronate (G) (M and G are isomers). The physical properties of alginate are typically dependent on the M/G ratio, G-content, and the average length of G blocks in the polymer.[37,38] Peaks of alginate were observed at 4.86 ppm (G-1), 4.58 ppm (G<u>G</u>M-5), 4.51 ppm (M<u>G</u>M-5), 4.45 ppm (<u>M</u>M-1), and 4.28 ppm (<u>G</u>G-5). Distinguished peaks of A-PNIPAAm appeared for alginate-*g*-PNIPAAm under the 2 ppm region, compared with that of alginate. These results indicated that alginate-*g*-PNIPAAm was successfully synthesized.

The DS of PNIPAAm to alginate was determined by elemental analysis. The DS values were 9.3 and 17.1 for DS 10 and DS 20 samples, respectively. These values were also confirmed by quantitative NMR analysis and were found to be 9.2 and 16.4 for DS 10 and DS 20 samples, respectively. The toxicity of alginate-*g*-PNIPAAm was evaluated using an EZ-Cytox cell viability assay kit and SCC-7 cells. Alginate-*g*-PNIPAAm did not show significant cytotoxicity (Figure S3). It has been often reported that NIPAAm monomers show significant cytotoxicity;[39] however, alginate-*g*-PNIPAAm was considered to be safe for further studies.

Micelle Formation of Alginate-*g*-PNIPAAm. Alginate-*g*-PNIPAAm formed self-assembled micelles in distilled water at 37 °C due to the increased hydrophobicity of PNIPAAm (Figure 2a,b). Self-assembling of alginate-*g*-PNIPAAm begins immediately at 37 °C and completes approximately 2 min postincubation (data now shown). The lower critical solution temperature (LCST) of alginate-*g*-PNIPAAm was slightly increased compared with that of A-PNIPAAm, but it was still close to human body temperature (Figure 2c). Micelles that formed at 37 °C dissolved when the temperature was decreased to 20 °C. However, when the temperature was increased to 37 °C again, the micelles reformed immediately, as confirmed by DLS studies (Figure 2d). Multiple size distribution curves of alginate-*g*-PNIPAAm micelles were displayed simultaneously to confirm temperature-dependent reversible micelle formation.

The mean diameter of the micelles was dependent on the PNIPAAm chain length and polymer concentration (Figure 3). Micelles that were prepared from alginate-*g*-PNIPAAm (MW$_{PNIPAAm}$ = 1 kDa) were approximately 400 nm in diameter with a narrow size distribution ([polymer] = 1 mg/mL) irrespective of the DS (Figure 3a). Increasing the molecular weight of PNIPAAm significantly increased the size of micelles. Alginate-*g*-PNIPAAm with MW$_{PNIPAAm}$ = 4 kDa and DS 20 could not be obtained due to undesired precipitation during the synthesis. Furthermore, the polymer concentration was also critical in controlling the micelle size (Figure 3b). Alginate-*g*-PNIPAAm micelles (MW$_{PNIPAAm}$ = 1 kDa; [polymer] = 0.5 mg/mL) were approximately 250 nm in diameter, which might
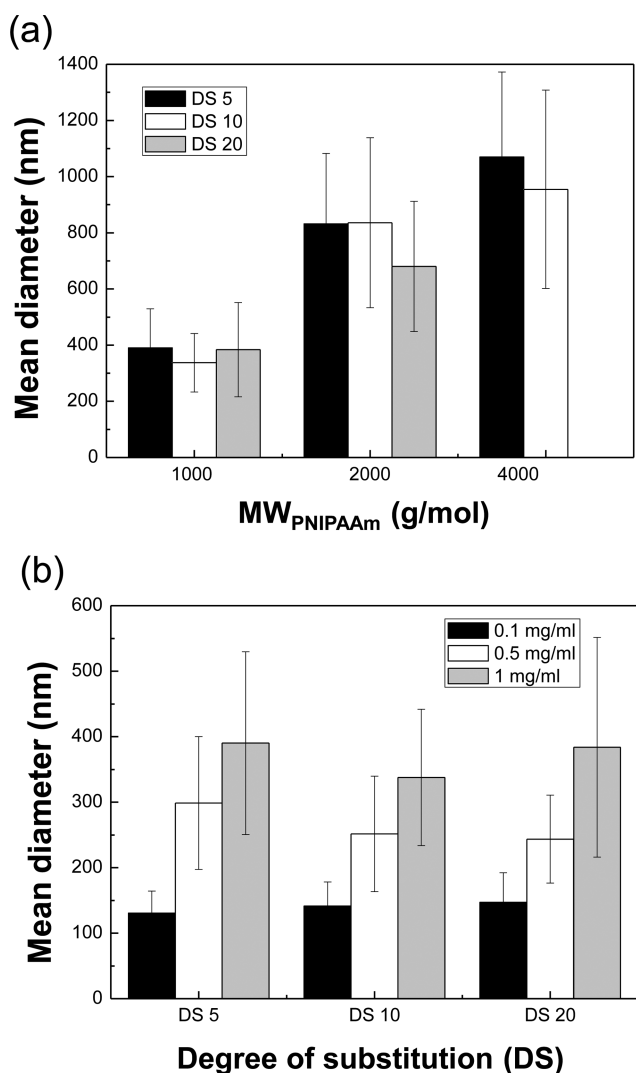
Figure 3. Effect of (a) PNIPAAm chain length ([polymer] = 1 mg/mL) and (b) polymer concentration (MW$_{PNIPAAm}$ = 1 kDa) on the size of alginate-g-PNIPAAm micelles in distilled water at 37 °C.

be an ideal size to render them useful as a delivery vehicle for anti-cancer drugs.

The CMC was determined from the plot of emission intensity ratio (I_1/I_3) of pyrene entrapped in alginate-g-PNIPAAm micelles vs polymer concentration. Pyrene has different photophysical characteristics depending on its surrounding hydrophilic and hydrophobic environments.[40,41] The CMC values of alginate-g-PNIPAAm were calculated as being between 0.04 and 0.12 mg/mL (Figure 4). The higher the DS, the lower the CMC values of the micelles. The relatively low CMC values of alginate-g-PNIPAAm micelles may be advantageous in terms of stability when the micelles are injected into the body and diluted with body fluids.

In Vitro Drug Release. DOX was loaded into alginate-g-PNIPAAm micelles using a dialysis method, and characteristics of DOX-loaded alginate-g-PNIPAAm micelles, such as mean diameter, encapsulation efficiency, and drug content, are shown in Table 1. No significant change in the mean diameter of micelles was observed for micelles with either DS 10 or DS 20 when the weight ratio of drug to polymer was 0.2. However, the size of DOX-loaded micelles was substantially increased at a drug-to-polymer ratio of 0.4. Alginate-g-PNIPAAm may form
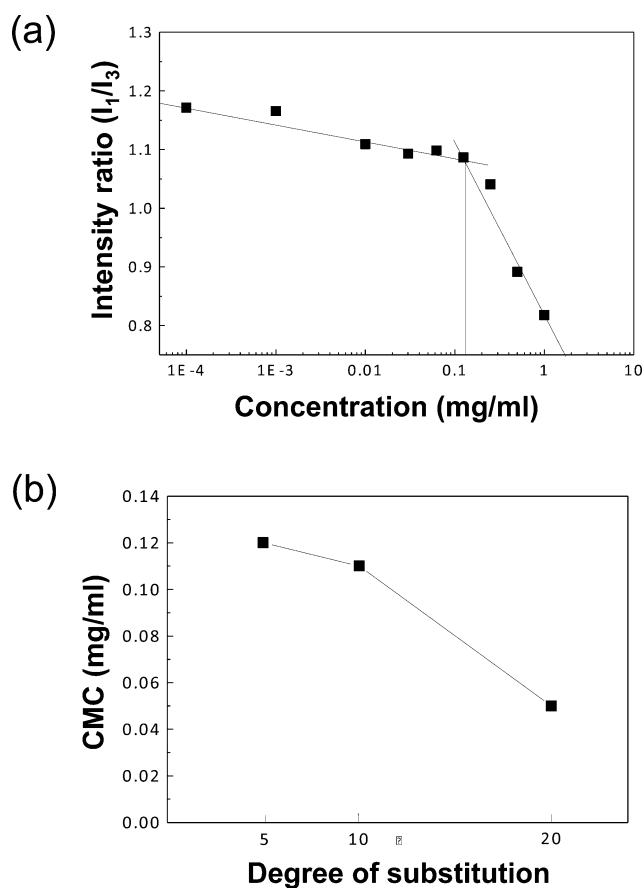

Figure 4. (a) Plot for the intensity ratio (I_1/I_3) determined from pyrene emission spectra vs alginate-g-PNIPAAm concentration at 37 °C (MW$_{PNIPAAm}$ = 1 kDa, DS 5). (b) Changes in the critical micelle concentration (CMC) of alginate-g-PNIPAAm micelles in distilled water at 37 °C as a function of DS.

Table 1. Characteristics of DOX-Loaded Alginate-g-PNIPAAm Micelles[a]

DS	drug/polymer (w/w)	mean diameter (nm)	encapsulation efficiency (%)	drug content (%)
10	0	252 ± 88		
	0.2	256 ± 94	62.7	12.5
	0.4	498 ± 266	60.4	24.2
20	0	244 ± 67		
	0.2	248 ± 81	58.2	11.6
	0.4	391 ± 175	59.9	24.0

[a][polymer] = 0.5 mg/mL; MW$_{PNIPAAm}$ = 1kD.

polymeric micelles with multiple hydrophobic cores at 37 °C due to the rigidity of the alginate backbone, like that for other polysaccharide-based micelles.[42] DOX can be incorporated into the hydrophobic cores, and the size of DOX-loaded micelles may significantly increase when the drug content reaches a certain value due to the existence of multiple cores and a lack of chain flexibility. All DOX-loaded alginate-g-PNIPAAm micelles had a similar encapsulation efficiency of approximately 60%. The cumulative release of DOX from alginate-g-PNIPAAm micelles was next monitored at 37 °C in vitro (Figure 5). The sustained release of DOX from the micelles was achieved for 96 h, and more than 90% of the DOX was released from micelles with DS 20. The release rate of DOX was not significantly influenced by the DS of PNIPAAm in alginate-g-PNIPAAm
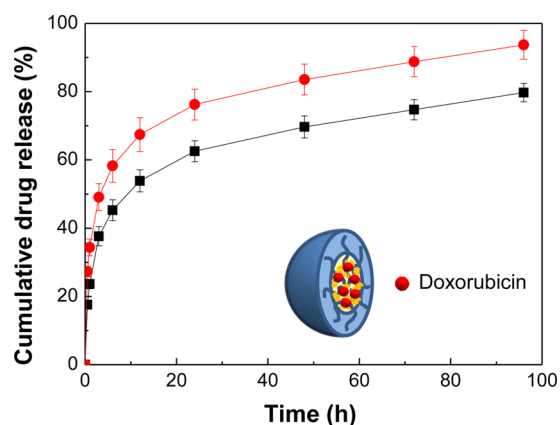
Figure 5. Cumulative release of doxorubicin from alginate-*g*-PNIPAAm micelles at 37 °C (■, DS10; ●, DS 20; drug/polymer = 0.4, weight ratio; [polymer] = 0.5 mg/mL; MW$_{PNIPAAm}$ = 1 kDa; n = 3).

micelles after the initial burst. Cell viability was significantly decreased when SCC7 cells were treated with DOX-loaded alginate-*g*-PNIPAAm micelles, which was similar to that of free DOX (Figure S4), indicating that DOX released from the micelles is effective in inducing cellular apoptosis. It might be advantageous that alginate-*g*-PNIPAAm forms micelles by simply increasing the temperature of a mixture solution of polymer and drug just before administration. Micelle formation from polymer amphiphiles often requires organic solvent or external physical force (e.g., ultrasound), and removal of the solvent is critical.[43,44] Alginate-*g*-PNIPAAm micelles may avoid this preparation step. However, these micelles are not temperature-responsive drug carriers and may release the loaded drug by diffusion above the LCST.[32]

In Vivo Tumor Targeting Ability of Alginate-*g*-PNIPAAm Micelles. The in vivo tumor-targeting ability of alginate-*g*-PNIPAAm micelles was evaluated using near-infrared fluorescent (NIRF) dye-conjugated micelles (dye/polymer = 1 w/w). NIRF dyes have been widely utilized in deep-tissue imaging because of their high penetration, low tissue absorption, and scattering.[45] No significant change in the diameter between dye-conjugated micelles (257 ± 91 nm) and nonconjugated micelles (244 ± 67 nm) was observed (DS 20; MW$_{PNIPAAm}$ = 1kD; [polymer] = 0.5 mg/mL). Dye-conjugated alginate-*g*-PNIPAAm micelles were injected intravenously into a tumor-bearing mouse model. Figure 6a shows real-time images of alginate-*g*-PNIPAAm micelles in the mouse model. A strong signal of free dye alone was observed 6 h postinjection, but the signal decreased over time. Interestingly, the use of alginate-*g*-PNIPAAm micelles enhanced the NIRF signals at the tumor site. These results may indicate that alginate-*g*-PNIPAAm micelles have a potential tumor targeting ability caused by the EPR effect and that the NIRF dye-conjugated polymer micelles can be used to visualize the tumor margin. Furthermore, ex vivo images of major organs and tumors dissected from the mice 48 h postinjection also demonstrated substantial accumulation of alginate-*g*-PNIPAAm micelles in the tumor (Figure 6c).

Micelles with higher DS showed more accumulation at the tumor site when intravenously injected into a tumor-bearing mouse model. This might be attributed to the enhanced structural stability of the micelles in the bloodstream, leading to enhanced accumulation at the tumor site.[46] Increasing the
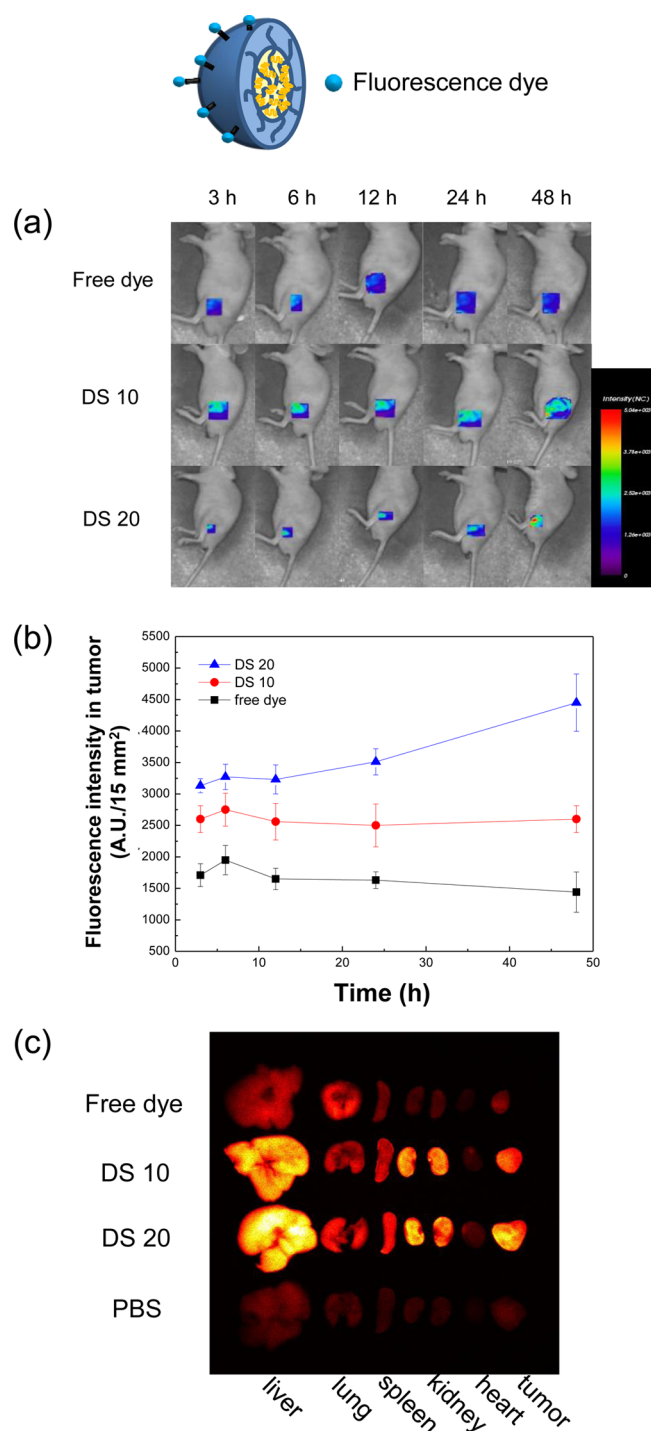
Figure 6. (a) Time-dependent, noninvasive in vivo images of dye-conjugated alginate-*g*-PNIPAAm micelles in a tumor-bearing mouse model and (b) changes in the fluorescence intensity over time. (c) Ex vivo images of major organs and tumors dissected from the mice 48 h postinjection ([polymer] = 0.5 mg/mL; MW$_{PNIPAAm}$ = 1 kDa; n = 3).

circulation time of micelles can be also achieved by modification with poly(ethylene glycol) (i.e., PEGylation), which enhances the EPR effect and resultant tumor accumulation, as previously reported in other systemic drug delivery systems.[47,48] It is relatively easy to load polymeric nanoparticles with multiple diagnostic agents,[49] suggesting that this multimodal imaging ability may facilitate their clinical use for cancer detection.
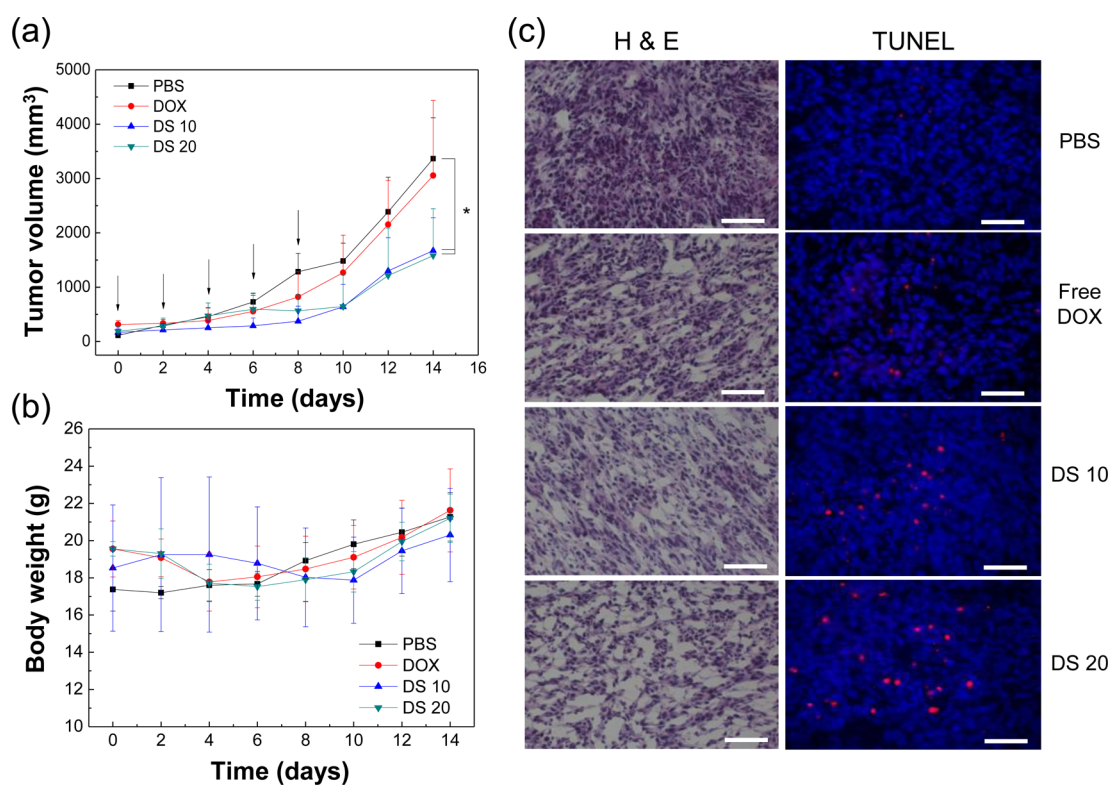
Figure 7. Changes in (a) tumor volume and (b) body weight of tumor-bearing mice treated with PBS, DOX, and DOX-loaded alginate-*g*-PNIPAAm micelles ([polymer] = 0.5 mg/mL; $MW_{PNIPAAm}$ = 1 kDa; drug/polymer = 0.4, weight ratio; *n* = 5) in a tumor-bearing mouse model ([DOX] = 1.2 mg/kg mouse). Arrows indicate when injections occurred. (c) Tissue sections were retrieved from the tumor-bearing mice and stained with H&E and TUNEL (scale bar, 50 μm). Red TUNEL signals indicate apoptotic cell death.

Cancer Therapeutic Effect. The in vivo anti-cancer efficacy of DOX-loaded alginate-*g*-PNIPAAm micelles was evaluated in a tumor-bearing mouse model. DOX-loaded micelles were intravenously injected at days 0, 2, 4, 6, and 8. The tumor volume and body weight of these mice were monitored for 14 days (Figure 7). The mice treated with PBS or DOX alone were also used as a control group (intravenous injection at days 0, 2, 4, 6, and 8). The tumor volume of mice that received PBS alone reached about 3500 mm³. The soluble DOX-treated group did not show significant difference in the tumor volume compared to that of PBS-treated group. Interestingly, the tumor volumes of mice treated with DOX-loaded micelles were greatly suppressed compared with those of the control groups (Figure 7a). Significant accumulation of DOX-loaded micelles at the tumor site may have enhanced the cancer therapeutic effect. This finding can be explained by the results obtained from in vivo tumor targeting studies (Figures 6). However, no significant difference in tumor volume was observed between mice treated with DOX-loaded micelles with DS 20 and mice treated with DOX-loaded micelles with DS 10, irrespective of their different tumor targeting ability. This might be due to the increased size of the DOX-loaded micelles compared with that of unloaded micelles (Table 1). This size change may have influenced the EPR effect of the micelles and their resultant tumor accumulation. However, DOX-loaded micelles showed strong potential in suppressing tumor growth compared to that of free DOX at the same dose.

No significant loss of body weight was observed for mice treated with DOX-loaded alginate-*g*-PNIPAAm micelles (Figure 7b), which may indicate reduced side effects of DOX when used with polymeric micelles. Compared with other previous reports, the amount of free DOX used in this study was relatively low,[50,51] and no significant therapeutic effects or side effects were observed. Tissue sections stained with H&E and TUNEL also supported the therapeutic efficacy of DOX-loaded alginate-*g*-PNIPAAm micelles (Figure 7c). Substantial tissue deficits were observed at the tumor site of mice treated with the micelles (H&E), indicating reduction in the number of tumor cells. Apoptotic cell nuclei (red TUNEL signals) were also clearly visible for mice treated with DOX-loaded alginate-*g*-PNIPAAm micelles compared with those treated with free DOX.

■ CONCLUSIONS

We demonstrated that alginate-*g*-PNIPAAm could form self-assembled micelles in water by simply changing the temperature and that the micelle formation was thermally reversible. The characteristics of micelles were dependent on the chain length of PNIPAAm, polymer concentration, and degree of substitution of PNIPAAm to alginate. The micelles had the ability to accumulate at the tumor site in a mouse model as a result of the EPR effect, which was confirmed using NIRF imaging. In addition, the enhanced therapeutic effect of DOX-loaded alginate-*g*-PNIPAAm micelles compared with that of free DOX was verified in a tumor-bearing mouse model. This approach to designing and tailoring polymeric micelles may provide a useful means for the development of various delivery vehicles suitable for cancer therapy.

■ ASSOCIATED CONTENT

⊚ Supporting Information

FT-IR and ¹H NMR data for alginate-*g*-PNIPAAm. Cytotoxicity of alginate-*g*-PNIPAAm and DOX released from the micelles. This material is available free of charge via the Internet at http://pubs.acs.org.

■ AUTHOR INFORMATION

Corresponding Author

*Tel.: +82-2-2220-0482; Fax: +82-2-2293-2642; E-mail: leeky@hanyang.ac.kr.

Notes

The authors declare no competing financial interest.

■ ACKNOWLEDGMENTS

■ REFERENCES

(1) Cheng, Z.; Al Zaki, A.; Hui, J. Z.; Muzykantov, V. R.; Tsourkas, A. Multifunctional Nanoparticles: Cost Versus Benefit of Adding Targeting and Imaging Capabilities. *Science* **2012**, *338*, 903−910.

(2) Gamboa, J. M.; Leong, K. W. In Vitro and in Vivo Models for the Study of Oral Delivery of Nanoparticles. *Adv. Drug Delivery Rev.* **2013**, *65*, 800−810.

(3) Koo, H.; Huh, M. S.; Ryu, J. H.; Lee, D.-E.; Sun, I.-C.; Choi, K.; Kim, K.; Kwon, I. C. Nanoprobes for Biomedical Imaging in Living Systems. *Nano Today* **2011**, *6*, 204−220.

(4) Petros, R. A.; DeSimone, J. M. Strategies in the Design of Nanoparticles for Therapeutic Applications. *Nat. Rev. Drug Discovery* **2010**, *9*, 615−627.

(5) Gabizon, A.; Shiota, R.; Papahadjopoulos, D. Pharmacokinetics and Tissue Distribution of Doxorubicin Encapsulated in Stable Liposomes with Long Circulation Times. *J. Natl. Cancer Inst.* **1989**, *81*, 1484−1488.

(6) Kwon, G. S.; Kataoka, K. Block Copolymer Micelles as Long-Circulating Drug Vehicles. *Adv. Drug Delivery Rev.* **1995**, *16*, 295−309.

(7) Nishiyama, N.; Kataoka, K. Current State, Achievements, and Future Prospects of Polymeric Micelles as Nanocarriers for Drug and Gene Delivery. *Pharmacol. Ther.* **2006**, *112*, 630−648.

(8) Kataoka, K.; Kwon, G. S.; Yokoyama, M.; Okano, T.; Sakurai, Y. Block Copolymer Micelles as Vehicles for Drug Delivery. *J. Controlled Release* **1993**, *24*, 119−132.

(9) Kataoka, K.; Harada, A.; Nagasaki, Y. Block Copolymer Micelles for Drug Delivery: Design, Characterization and Biological Significance. *Adv. Drug Delivery Rev.* **2001**, *47*, 113−131.

(10) Matsumura, Y.; Hamaguchi, T.; Ura, T.; Muro, K.; Yamada, Y.; Shimada, Y.; Shirao, K.; Okusaka, T.; Ueno, H.; Ikeda, M.; Watanabe, N. Phase I Clinical Trial and Pharmacokinetic Evaluation of Nk911, a Micelle-Encapsulated Doxorubicin. *Br. J. Cancer* **2004**, *91*, 1775−1781.

(11) Fang, J.; Nakamura, H.; Maeda, H. The EPR Effect: Unique Features of Tumor Blood Vessels for Drug Delivery, Factors Involved, and Limitations and Augmentation of the Effect. *Adv. Drug Delivery Rev.* **2011**, *63*, 136−151.

(12) Lee, K. Y.; Mooney, D. J. Alginate: Properties and Biomedical Applications. *Prog. Polym. Sci.* **2012**, *37*, 106−126.

(13) Cheng, Y.; Yu, S.; Zhen, X.; Wang, X.; Wu, W.; Jiang, X. Alginic Acid Nanoparticles Prepared through Counterion Complexation Method as a Drug Delivery System. *ACS Appl. Mater. Interfaces* **2012**, *4*, 5325−5332.

(14) Brudno, Y.; Silva, E. A.; Kearney, C. J.; Lewin, S. A.; Miller, A.; Martinick, K. D.; Aizenberg, M.; Mooney, D. J. Refilling Drug Delivery Depots through the Blood. *Proc. Natl. Acad. Sci. U.S.A.* **2014**, *111*, 12722−12727.

(15) Ribeiro, A. J.; Neufeld, R. J.; Arnaud, P.; Chaumeil, J. C. Microencapsulation of Lipophilic Drugs in Chitosan-Coated Alginate Microspheres. *Int. J. Pharm.* **1999**, *187*, 115−123.

(16) Takeuchi, H.; Yasuji, T.; Hino, T.; Yamamoto, H.; Kawashima, Y. Spray-Dried Composite Particles of Lactose and Sodium Alginate for Direct Tabletting and Controlled Releasing. *Int. J. Pharm.* **1998**, *174*, 91−100.

(17) Tønnesen, H. H.; Karlsen, J. Alginate in Drug Delivery Systems. *Drug Dev. Ind. Pharm.* **2002**, *28*, 621−630.

(18) Bae, K. H.; Choi, S. H.; Park, S. Y.; Lee, Y.; Park, T. G. Thermosensitive Pluronic Micelles Stabilized by Shell Cross-Linking with Gold Nanoparticles. *Langmuir* **2006**, *22*, 6380−6384.

(19) Chung, J. E.; Yokoyama, M.; Okano, T. Inner Core Segment Design for Drug Delivery Control of Thermo-Responsive Polymeric Micelles. *J. Controlled Release* **2000**, *65*, 93−103.

(20) Jun, Y. J.; Toti, U. S.; Kim, H. Y.; Yu, J. Y.; Jeong, B.; Jun, M. J.; Sohn, Y. S. Thermoresponsive Micelles from Oligopeptide-Grafted Cyclotriphosphazenes. *Angew. Chem., Int. Ed.* **2006**, *45*, 6173−6176.

(21) Kim, I.-S.; Jeong, Y.-I.; Cho, C.-S.; Kim, S.-H. Thermo-Responsive Self-Assembled Polymeric Micelles for Drug Delivery in Vitro. *Int. J. Pharm.* **2000**, *205*, 165−172.

(22) Schild, H. G. Poly(*N*-isopropylacrylamide): Experiment, Theory and Application. *Prog. Polym. Sci.* **1992**, *17*, 163−249.

(23) Maeda, Y.; Higuchi, T.; Ikeda, I. Change in Hydration State During the Coil-Globule Transition of Aqueous Solutions of Poly(*N*-isopropylacrylamide) as Evidenced by FTIR Spectroscopy. *Langmuir* **2000**, *16*, 7503−7509.

(24) Cammas, S.; Suzuki, K.; Sone, C.; Sakurai, Y.; Kataoka, K.; Okano, T. Thermo-Responsive Polymer Nanoparticles with a Core−Shell Micelle Structure as Site-Specific Drug Carriers. *J. Controlled Release* **1997**, *48*, 157−164.

(25) Smith, L.; Cornelius, V.; Plummer, C.; Levitt, G.; Verrill, M.; Canney, P.; Jones, A. Cardiotoxicity of Anthracycline Agents for the Treatment of Cancer: Systematic Review and Meta-Analysis of Randomised Controlled Trials. *BMC Cancer* **2010**, *10*, 337.

(26) Soledad Lencina, M. M.; Iatridi, Z.; Villar, M. A.; Tsitsilianis, C. Thermoresponsive Hydrogels from Alginate-Based Graft Copolymers. *Eur. Polym. J.* **2014**, *61*, 33−44.

(27) Dumitriu, R. P.; Mitchell, G. R.; Vasile, C. Multi-Responsive Hydrogels Based on *N*-Isopropylacrylamide and Sodium Alginate. *Polym. Int.* **2011**, *60*, 222−233.

(28) Tan, R. W.; She, Z. D.; Wang, M. B.; Fang, Z.; Liu, Y. S.; Feng, Q. L. Thermo-Sensitive Alginate-Based Injectable Hydrogel for Tissue Engineering. *Carbohydr. Polym.* **2012**, *87*, 1515−1521.

(29) Prabaharan, M.; Mano, J. F. Stimuli-Responsive Hydrogels Based on Polysaccharides Incorporated with Thermo-Responsive Polymers as Novel Biomaterials. *Macromol. Biosci.* **2006**, *6*, 991−1008.

(30) Zschoche, S.; Rueda, J.; Boyko, V.; Krahl, F.; Arndt, K. F.; Voit, B. Thermo-Responsive Nanogels Based on Poly[NIPAAm-graft-(2-alkyl-2-oxazoline)]s Crosslinked in the Micellar State. *Macromol. Chem. Phys.* **2010**, *211*, 1035−1042.

(31) Topp, M. D. C.; Dijkstra, P. J.; Talsma, H.; Feijen, J. Thermosensitive Micelle-Forming Block Copolymers of Poly(ethylene glycol) and Poly(*N*-isopropylacrylamide). *Macromolecules* **1997**, *30*, 8518−8520.

(32) Rapoport, N. Physical Stimuli-Responsive Polymeric Micelles for Anti-cancer Drug Delivery. *Prog. Polym. Sci.* **2007**, *32*, 962−990.

(33) Pai, V. B.; Nahata, M. C. Cardiotoxicity of Chemotherapeutic Agents: Incidence, Treatment and Prevention. *Drug Saf.* **2000**, *22*, 263−302.

(34) Kratz, F. Albumin as a Drug Carrier: Design of Prodrugs, Drug Conjugates and Nanoparticles. *J. Controlled Release* **2008**, *132*, 171−183.

(35) Kim, K.; Kim, J. H.; Park, H.; Kim, Y.-S.; Park, K.; Nam, H.; Lee, S.; Park, J. H.; Park, R.-W.; Kim, I.-S. Tumor-Homing Multifunctional Nanoparticles for Cancer Theragnosis: Simultaneous Diagnosis, Drug Delivery, and Therapeutic Monitoring. *J. Controlled Release* **2010**, *146*, 219−227.

(36) Nakajima, N.; Ikada, Y. Mechanism of Amide Formation by Carbodiimide for Bioconjugation in Aqueous Media. *Bioconjugate Chem.* **1995**, *6*, 123−130.

(37) Draget, K. I.; Skjåk Bræk, G.; Smidsrød, O. Alginic Acid Gels: The Effect of Alginate Chemical Composition and Molecular Weight. *Carbohyd. Polym.* **1994**, *25*, 31−38.

(38) Santi, C.; Coppetta, D.; Santoro, S.; Basta, G.; Montanucci, P.; Racanicchi, L.; Calafiore, R. NMR Analysis of Non Hydrolyzed Samples of Sodium Alginate. *Proc. ECSOC-12, Int. Electron. Conf. Synth. Org. Chem., 12th* **2008**, 1−10.

(39) Wadajkar, A. S.; Koppolu, B.; Rahimi, M.; Nguyen, K. T. Cytotoxic Evaluation of N-Isopropylacrylamide Monomers and Temperature-Sensitive Poly (*N*-isopropylacrylamide) Nanoparticles. *J. Nanopart. Res.* **2009**, *11*, 1375−1382.

(40) Jiang, G.-B.; Quan, D.; Liao, K.; Wang, H. Preparation of Polymeric Micelles Based on Chitosan Bearing a Small Amount of Highly Hydrophobic Groups. *Carbohydr. Polym.* **2006**, *66*, 514−520.

(41) Astafieva, I.; Zhong, X. F.; Eisenberg, A. Critical Micellization Phenomena in Block Polyelectrolyte Solutions. *Macromolecules* **1993**, *26*, 7339−7352.

(42) Lee, K. Y.; Jo, W. H.; Kwon, I. C.; Kim, Y.-H.; Jeong, S. Y. Structural Determination and Interior Polarity of Self-aggregates Prepared from Deoxycholic Acid-Modified Chitosan in Water. *Macromolecules* **1998**, *31*, 378−383.

(43) Kim, S.; Kim, J. Y.; Huh, K. M.; Acharya, G.; Park, K. Hydrotropic Polymer Micelles Containing Acrylic Acid Moieties for Oral Delivery of Paclitaxel. *J. Controlled Release* **2008**, *132*, 222−229.

(44) Thambi, T.; Yoon, H. Y.; Kim, K.; Kwon, I. C.; Yoo, C. K.; Park, J. H. Bioreducible Block Copolymers Based on Poly(ethylene glycol) and Poly(gamma-benzyl L-glutamate) for Intracellular Delivery of Camptothecin. *Bioconjugate Chem.* **2011**, *22*, 1924−1931.

(45) Peng, L.; Liu, R.; Marik, J.; Wang, X.; Takada, Y.; Lam, K. S. Combinatorial Chemistry Identifies High-Affinity Peptidomimetics against $\alpha 4\beta 1$ Integrin for in Vivo Tumor Imaging. *Nat. Chem. Biol.* **2006**, *2*, 381−389.

(46) Na, J. H.; Lee, S. Y.; Lee, S.; Koo, H.; Min, K. H.; Jeong, S. Y.; Yuk, S. H.; Kim, K.; Kwon, I. C. Effect of the Stability and Deformability of Self-assembled Glycol Chitosan Nanoparticles on Tumor-Targeting Efficiency. *J. Controlled Release* **2012**, *163*, 2−9.

(47) Harris, J. M.; Chess, R. B. Effect of Pegylation on Pharmaceuticals. *Nat. Rev. Drug Discovery* **2003**, *2*, 214−221.

(48) Owens, D. E., III; Peppas, N. A. Opsonization, Biodistribution, and Pharmacokinetics of Polymeric Nanoparticles. *Int. J. Pharm.* **2006**, *307*, 93−102.

(49) Lee, D.-E.; Koo, H.; Sun, I.-C.; Ryu, J. H.; Kim, K.; Kwon, I. C. Multifunctional Nanoparticles for Multimodal Imaging and Theragnosis. *Chem. Soc. Rev.* **2012**, *41*, 2656−2672.

(50) Gabizon, A.; Tzemach, D.; Mak, L.; Bronstein, M.; Horowitz, A. T. Dose Dependency of Pharmacokinetics and Therapeutic Efficacy of Pegylated Liposomal Doxorubicin (Doxil) in Murine Models. *J. Drug Targeting* **2002**, *10*, 539−548.

(51) Keith, W. N.; Mee, P. J.; Brown, R. Response of Mouse Skin Tumors to Doxorubicin Is Dependent on Carcinogen Exposure. *Cancer Res.* **1990**, *50*, 6841−6847.